Journal of the European Ceramic Society 19 (1999) 1115–1118

PII: S0955-2219(98)00385-9
0955-2219/99/$ - see front matter

Raman Scattering and X-ray Diffraction Investigations of Sol–Gel Derived SBN Powders

Melanie M. T. Ho, C. L. Mak* and K. H. Wong

Department of Applied Physics and Materials Research Center, The Hong Kong Polytechnic University, Hung Hom, Hong Kong

Abstract

Sol–gel derived $Sr_xBa_{1-x}Nb_2O_6$ (SBN) powders were prepared at an annealing temperature of 1200°C. Their structural changes were characterized by Raman spectroscopy and X-ray diffractometry. Changes in the peak position and the relative intensity of the Raman spectra and X-ray patterns were examined for different values of x. *Our results suggest that the SBN powders consist of a mixture of orthorhombic phase $BaNb_2O_6$ (BN) and tetragonal tungsten-bronze phase (TTB) SBN powders for* $x < 0{\cdot}5$, *and orthorhombic phase $SrNb_2O_6$ (SN) and TTB phase SBN powders for* $x > 0{\cdot}5$. *Pure TTB type SBN powders with* $x \neq 0{\cdot}5$, *however, were obtained at higher annealing temperatures. A possible formation route of the sol–gel derived SBN powder is discussed.* © *1999 Elsevier Science Limited. All rights reserved*

Keywords: strontium barium niobate, sol–gel processes, spectroscopy, X-ray methods, dielectric properties.

1 Introduction

SBN is a well known solid solution of SN and BN with a general formula of $Sr_xBa_{1-x}Nb_2O_6$. Owing to its rather large pyroelectric and electro-optic coefficients of $31\times10^{-2}\,\mu C\,cm^{-2}\,K^{-1}$ and $41\times10^{-12}\,m\,V^{-1}$ respectively,[1] SBN has attracted a great deal of attention recently and is currently being investigated as a potential material for pyroelectric, electro-optics and photorefractive devices.[2]

SN and BN have crystal structures of type I and type II orthorhombic structure, respectively.[3] SBN, on the other hand, exhibits TTB structure with its ferroelectric polar axis along the *c*-direction for $0{\cdot}25 \leq x \leq 0{\cdot}75$.[1] Its Curie temperature, T_c, changes linearly with x (T_c increases from $T_c \approx 57°C$ at $x = 0{\cdot}75$ to $T_c \approx 247°C$ at $x = 0{\cdot}25$). Other physical properties of SBN also vary with its composition.[1,4] For example, single crystal SBN25 ($x = 0{\cdot}25$) has a low dielectric constant ($\varepsilon_{33}/\varepsilon_0 = 118$) while single crystal SBN75 has a very large dielectric constant ($\varepsilon_{33}/\varepsilon_0 = 3400$).[1] Therefore, SBN with varies composition are of importance in respect to different applications.

In this paper, we report on the fabrication of SBN powders with good dielectric properties using the sol–gel method. The dielectric constant of these SBN powders was measured as a function of x. The measured x-dependence of the dielectric constant, however, did not match with those observed in single crystal. In order to elucidate these discrepancy, the structural properties of these SBN powders with varied x were measured using Raman spectroscopy (RS) and X-ray diffractometry (XRD). A possible formation mechanism of sol–gel derived SBN powder is proposed.

2 Experimental

The starting agents for preparing the individual precursors were strontium metal, barium metal and niobium chloride. 2-methoxyethanol was used as both the common solvent and the stabilizing agent.[5,6] These three alkoxide precursors were thoroughly mixed according to the desired stoichiometric ratio and refluxed for 1 h. Amorphous powder could be produced by deliberately adding water into the SBN sol for hydrolysis and polycondensation, followed by drying at 100°C overnight. The as-prepared powders were then annealed at 1200°C in air for 2 h. In this study, $Sr_xBa_{1-x}Nb_2O_6$ powders with $x = 0$, 0·3, 0·5, 0·6, 0·75, 0·8 and 1 were prepared.

For dielectric measurements, the powders were pressed into circular pellets (radius = 3 mm and average thickness ~0·9 mm). Dielectric constant

*To whom correspondence should be addressed. Fax: +852-2333-7629; e-mail: apaclmak@polyu.edu.hk

and loss factors were measured in the 1 KHz and 10 MHz ranges with an impedance gain analyzer (HP 4194A). The crystallization behavior of SBN powders was characterized by XRD (Philips PW3710) analysis using Cu-K_α radiation. The chemical composition was confirmed by energy dispersive X-ray spectroscopy. Raman spectra for the powders were excited by 488 nm laser light from a CW argon gas laser (Coherent Innova 70). The laser power was kept at 50 mW to avoid laser annealing of the samples. All measurements were performed at room temperature. A 55 mm f/1.8 lens was used for collecting the scattered light which was dispersed and detected using a double grating monochromator (Spex 1403) equipped with a cooled photomultiplier tube (Hamamatsu R928). All spectra were recorded in the small-angle scattering geometry. The resolution obtained could be as good as 0·1 cm^{-1}.

3 Results and Discussion

Figure 1 shows the dielectric constant and loss factor of SBN powders as a function of x. It is seen that the dielectric constant has a maximum at $x = 0{\cdot}5$. These results contradict those reported for single crystal SBN,[1] in which the dielectric constant decreases with x for $0{\cdot}25 < x < 0{\cdot}75$. Figure 2(a) shows the unpolarized Raman spectrum in the vicinity of the optical phonon frequencies for single crystal $Sr_{0.6}Ba_{0.4}Nb_2O_6$ (SBN60). Similar to the spectrum given by Amzallag *et al.*,[7] two broad and strong A_1(TO) phonons at 260 and 635 cm^{-1}, one weak B_1(TO) phonon at 155 cm^{-1}, and one weak B_2 phonon at 420 cm^{-1} are observed. Since there are 132 optical phonon modes in the unit cell, it is possible that several nearly degenerate modes may occur and appear as one band. This degeneracy would contribution to the broadening of the band and asymmetric line-shape. Figure 2(b) and 2(f) shows the spectra of BN and SN, respectively. The spectra of SN and BN, which carry far more features than the spectrum of single crystal SBN, are similar to the spectra reported by Repelin.[3] The observed external A_1 mode in BN is smaller than that in SN because of the heavier mass of the metal cations in BN. As $x = 0{\cdot}8$, the SBN spectrum is similar to SN except that the peaks become broader with the evolution of two broad underneath features around 250 and 650 cm^{-1}. These broad features become more prominent while the SN peaks get weaker as x decreased to 0·75 [Fig. 2(e)]. As $x = 0{\cdot}5$, the spectrum [Fig. 2(d)] is identical to the TTB phase SBN single crystal except that the phonon peaks are broader. As x is further reduced to 0·3 [Fig. 2(c)], the two broad features with individual phonon peaks, which resemble phonons in BN, are observed. These findings indicate that for $x < 0{\cdot}5$, the powders consist of a mixture of TTB phase SBN and BN powders, and as $x > 0{\cdot}5$, the powders are composed of mixed TTB phase SBN and SN powders. However, for $x = 0{\cdot}5$, the powders are mainly single TTB phase SBN powders.

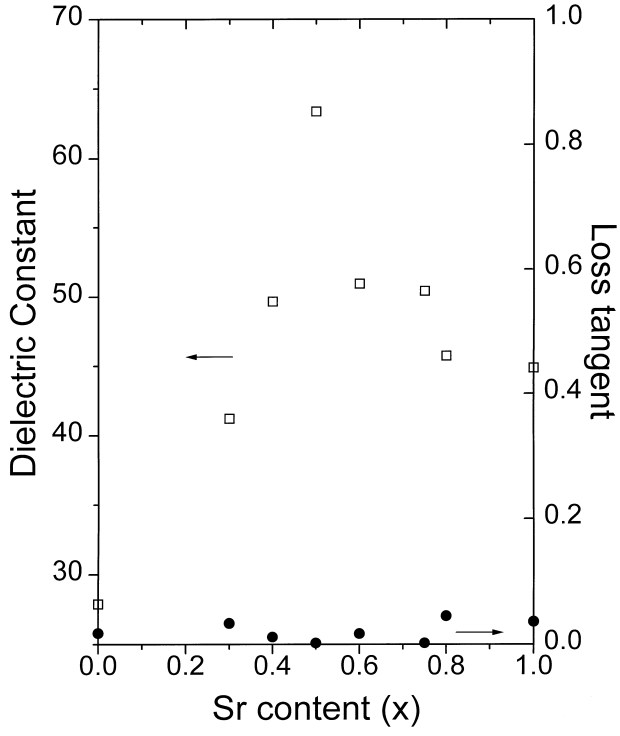

Fig. 1. Dielectric constant and loss factor of sol–gel derived $Sr_xBa_{1-x}Nb_2O_6$ powders measured at 10 MHz.

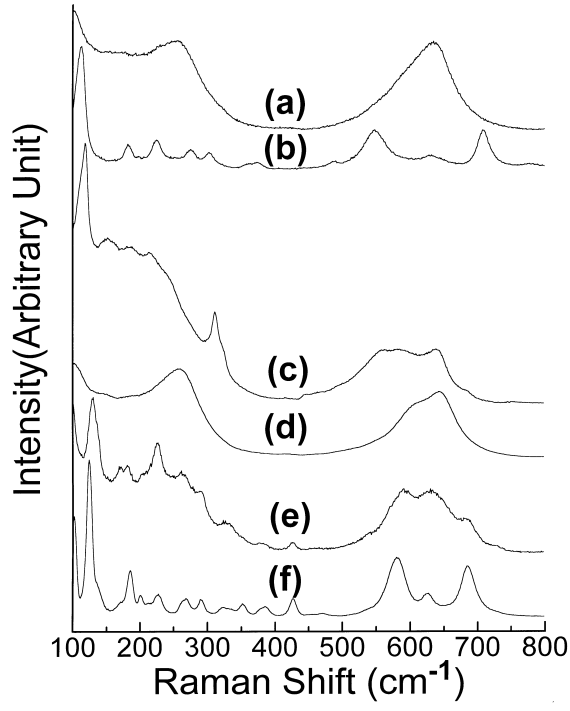

Fig. 2. The Raman spectra of SBN powders with (a) single crystal SBN60; (b) BN; (c) SBN30; (d) SBN50; (e) SBN75, and (f) SN.

In addition to RS, XRD was also employed to study the structural changes in these samples. Figure 3 shows the XRD patterns of SBN powders annealed at 1200°C for various Ba/Sr ratios. Using Scherrer's relation[8] which assumes the small crystallite size causing line broadening, we have obtained an average crystallite size of ~25 nm for all of our samples. Pure SN [Fig. 3(e)] shows a strong peak at $2\theta = 29{\cdot}1°$ while BN [Fig. 3(a)] exhibits two characteristic peaks at $2\theta = 28{\cdot}4°$ and 29·8°. For $x = 0{\cdot}5$ [Fig. 3(c)], a XRD pattern of single TTB phase SBN is obtained. This XRD pattern is consistent with that reported by Van-Damme *et al.*[4] As $0{\cdot}8 > x > 0{\cdot}5$ [Fig. 3(d)], the spectra contain a SBN-liked XRD pattern with the additional feature at $2\theta = 29{\cdot}1°$. This extra feature becomes stronger as x increases. The origin of this feature appears to arise from the SN phase. Similar to that observed in Raman spectra, this result indicates that at $x > 0{\cdot}5$, a mixture of TTB phase SBN and SN are present. The XRD peaks intensity ratios SN/SBN increased with increasing mole ratio of strontium. For $x = 0{\cdot}3$, however, the X-ray spectrum suggests the presence of a mixture of TTB phase SBN and BN.

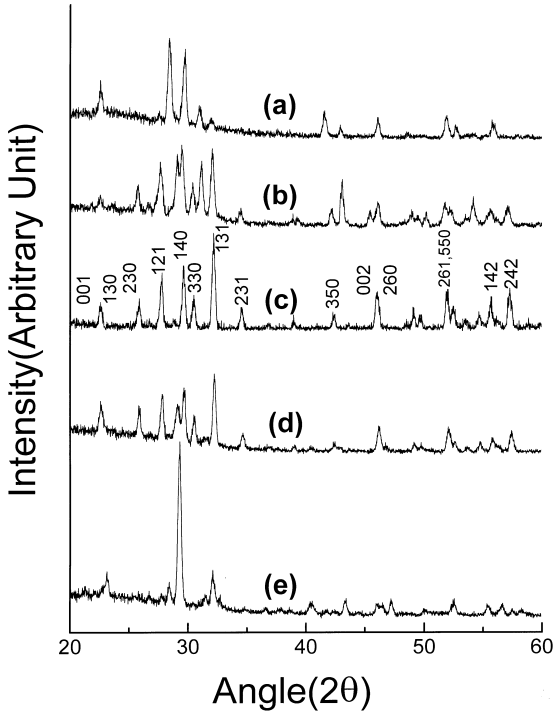

Fig. 3. The XRD pattern of SBN powders with (a) BN; (b) SBN30; (c) SBN50; (d) SBN75, and (e) SN.

In order to better understand the formation route of sol–gel derived SBN powders, we studied the evolution of structural properties of SBN60 powders as a function of annealing temperature. Figure 4(a) and (b) shows the Raman and XRD spectra of SBN60 powders annealed at various temperatures, respectively. At low annealing temperature, the Raman spectrum is SN-like. As the annealing temperature is increased, the phonon peaks become broader with the evolution of two broad underneath features around 250 and 650 cm^{-1}. These broad features become more noticeable while the SN peaks get weaker at higher annealing temperature. At 1400°C, the spectrum is essentially the same as the TTB phase SBN60 single crystal. Similar features are obtained in the XRD pattern, where the characteristic SN peak at $2\theta = 29{\cdot}1°$ diminishes as the annealing temperature is increased to 1400°C. Therefore we believe that the formation of SBN consists of two parallel reaction processes of BN and SN at low temperatures, and thereafter these two phases form a solid solution of SBN at a much higher temperature. From Figs 2 and 3, the intensity ratios SN/SBN are observed to increase with increasing mole ratio of strontium. This result indicates that the temperature for a complete formation of the TTB phase

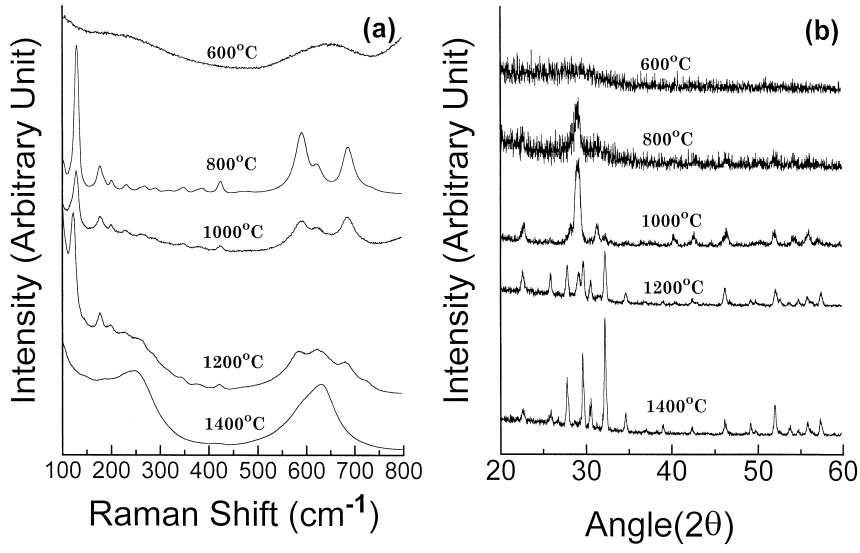

Fig. 4. The Raman spectra and XRD pattern of SBN60 powders annealed at different temperature.

SBN is higher with larger x. This evidence is consistent with the findings in SBN powder prepared by the mixed-oxide route.[9] According to the above scheme, the SBN (with $x > 0{\cdot}5$) powders annealed at 1200°C contain TTB phase SBN and an unwanted SN phase. It is this unwanted SN phase, which has a much lower dielectric constant, that degrades the dielectric properties of our SBN powders.

4 Conclusions

Structural changes of sol–gel derived SBN powders were studied using RS and XRD. Our results suggest that at annealing temperature = 1200°C, the SBN powders are a mixture of BN and TTB phase SBN for $x < 0{\cdot}5$, and SN and TTB phase SBN for $x > 0{\cdot}5$. Pure TTB phase SBN powders with $x \neq 0{\cdot}5$ could only be obtained at higher annealing temperatures. The formation of SBN seems to consist of two parallel reaction processes of BN and SN, and thereafter these two phases form a solid solution of SBN at a higher annealing temperature.

Acknowledgements

The work described in this paper was partially supported by a grant from the Research Grants Council of the Hong Kong Special Administrative Region (Project Q165). MTH was supported by M.Phil studentship of the Hong Kong Polytechnic University.

References

1. Xu, Y. *Ferroelectric Materials and Their Applications*. North Holland, Amsterdam, 1991, pp. 254–262.
2. Prokhorov, A. M. and Kuzminov, Y. S., *Ferroelectric Crystals for Laser Radiation Control*. Adam Hilger, Bristol, 1990, pp. 81–149.
3. Repelin, Y., Husson, E. and Brusset, H., Etude par spectroscopies d'absorption i.r. et de diffusion Raman des composés $A^{II}B_2O_6$ de structure de type "blocs 1×2"-I. Etude du niobate de baryum $BaNb_2O_6$. *Spectrochimica Acta*, 1979, **35**, 937–948.
4. VanDamme, N. S., Sutherland, A. E., Jones, L., Bridger, K. and Winzer, S. R., Fabrication of optically transparent and electrooptic strontium barium niobate ceramics. *J. Am. Ceram. Soc.*, 1991, **74**, 1785–1792.
5. Luk, C. H., Mak, C. L. and Wong, K. H., Characterization of strontium barium niobate films prepared by sol–gel process using 2-methoxyethanol. *Thin Solid Films*, **298**, 57–61.
6. Mak, L., Luk, C. H. and Wong, K. H., Thickness dependence of the structural properties of sol–gel derived $Sr_{0{\cdot}6}Ba_{0{\cdot}4}Nb_2O_4$ films. *Thin Solid Film*, 1998, **325**, 79–82.
7. Amzallag, E., Chang, T. S. and Pantell, R. H., Raman scattering by $Sr_xBa_{1-x}Nb_2O_6$. *J. Appl. Phys.*, 1971, **42**, 3254.
8. Cullity, B. D., *Elements of X-ray Diffraction*. Addison–Wesley, New York 1956, pp. 96–99.
9. Fang, T. T., Wu, N. T. and Shiau, F. S., Formation mechanism of strontium barium niobate ceramic powders. *J. Mater. Sci. Lett.*, 1994, **13**, 1746–1748.